

Review

Gold Nanoparticles as the Catalyst of Single-Walled Carbon Nanotube Synthesis

Yoshikazu Homma

Department of Physics, Tokyo University of Science, Shinjuku, Tokyo 162-8601, Japan;

E-Mail: homma@rs.tus.ac.jp; Tel.: +81-3-5228-8244; Fax: +81-3-5261-1023

Received: 29 July 2013; in revised form: 20 February 2014 / Accepted: 24 February 2014 /

Published: 5 March 2014

Abstract: Gold nanoparticles have been proven to act as efficient catalysts for chemical reactions, such as oxidation and hydrogen production. In this review we focus on a different aspect of the catalysis of gold nanoparticles; single-walled carbon nanotube (SWCNT) synthesis. This is not a traditional meaning of catalytic reaction, but SWCNTs cannot be synthesized without nanoparticles. Previously, gold was considered as unsuitable metal species as the catalyst of SWCNT synthesis. However, gold nanoparticles with diameters smaller than 5 nm were found to effectively produce SWCNTs. We discuss the catalysis of gold and related metals for SWCNT synthesis in comparison with conventional catalysts, such as iron, cobalt, and nickel.

Keywords: chemical vapor deposition; carbon nanotubes; graphene; growth mechanism

1. Introduction

Graphene is a monolayer material composed of six membered rings of sp^2 hybridized carbon atoms [1]. A single walled carbon nanotube (SWCNT) is a nano-scale cylinder composed of rolled-up graphene [1,2]. Due to their excellent mechanical strength and the chemical stability of the honeycomb structure of sp^2 carbon atoms, as well as their peculiar electric properties due to low dimensionality, graphene and SWCNT are intensively studied for future applications. For the formation of these nanocarbon materials, metal surfaces play an important role. Catalytic reaction is necessary for decomposition of hydrocarbons or alcohols that are used as the carbon feedstock in vapor deposition of nanocarbons. In addition, the (111) face of face-centered cubic (fcc) or the (0001) face of hexagonal closed packed (hcp), both of which take the triangular lattice of the highest surface atom density,

commensurate with the graphene lattice [3]. Furthermore, formation of the cylindrical structure of SWCNT requires a nanoparticle of, in most cases, metals. Thus, those metals, used for graphene and SWCNT synthesis, are called catalysts, especially in the case of SWCNTs.

Catalyst species mostly used for SWCNT synthesis are iron-group metals; iron (Fe), cobalt (Co), and nickel (Ni) [4], which have been known to have a catalytic function to assist carbon feedstock cracking and produce graphite layer on the bulk material surface [5]. For these species, a widely-accepted growth model is based on the vapor-liquid-solid (VLS) mechanism as the analogy of semiconductor nanowire growth from gold eutectic alloy [6,7]. During vapor phase growth, carbon bearing molecules are catalytically decomposed on the surface of the catalyst, which was supposed to be in a liquid phase due to the nano-size effect, resulting in the dissolution of carbon atoms into the catalyst particle. On supersaturation of carbon concentration in the particle, carbon atoms precipitate from the catalyst, leading to the formation of tubular carbon networks around or on the catalyst. From the viewpoint of carbon solubility and carbon eutectic alloy phase in the carbon-metal binary phase diagram, Fe, Co, and Ni are the elements capable of catalyzing SWCNT growth.

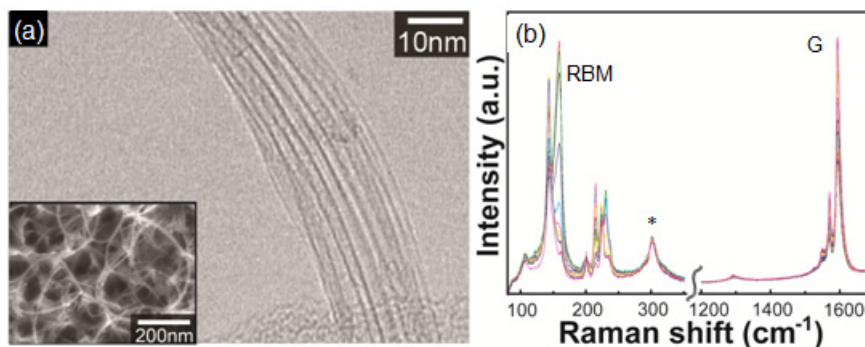
For high temperature synthesis methods, *i.e.*, arc discharge and laser aeration methods, other metal species, such as palladium (Pd) or platinum (Pt), were used [8]. On the other hand, gold (Au), silver (Ag), and copper (Cu) were considered unlikely to produce SWCNTs due to their low affinity to carbon [9]. This was proven to be incorrect by the findings of SWCNT growth from Au, Cu, and Ag almost simultaneously published from December, 2006, to January, 2007 [10–12]. Although many other species, including nonmetallic catalysts, have been reported to produce SWCNTs since then, Au, Cu, and Ag are particularly interesting because of their prominent difference in the affinity to carbon from iron group metals. Furthermore, Cu is now used as the substrate for monolayer graphene synthesis: due to the low carbon solubility, multilayer graphene is hard to form on the Cu surface [13]. As the underlying mechanism should be the same for graphene and SWCNTs, investigation of graphene growth would shed new light on SWCNT growth.

In this review, we focus on SWCNT synthesis by chemical vapor deposition (CVD) with Au and related metal catalysts. Among SWCNT synthesis methods, CVD is widely used for the SWCNT synthesis on the substrate, which is important for device applications and vertically or horizontally aligned SWCNT growth. The SWCNT growth is compared with those using conventional metal catalysts and the growth mechanism and controlled growth of SWCNTs are reviewed.

2. SWCNT Synthesis

Au had attracted an attention as the catalyst of SWCNT growth because semiconductor nanowires could be grown using Au nanoparticles [14]. However, before 2006, no reports could be found concerning SWCNT growth from Au. Lee *et al.* reported multilayered carbon nanotube (MWCNT) growth using Au nanoparticles on a SiO₂-Al₂O₃ support with acetylene as the carbon source [15]. The products were mostly defective carbon nanofilaments and some were MWCNTs with outer diameters of 13–25 nm. The Au particles were prepared by the liquid-phase reduction method using HAuCl₄ 4H₂O aqueous solution and dodecanethiol as a protective agent. The Au nanoparticles initially had average diameter of 1.66 nm before calcination, but agglomerated to form 10-nm-sized particles after calcination.

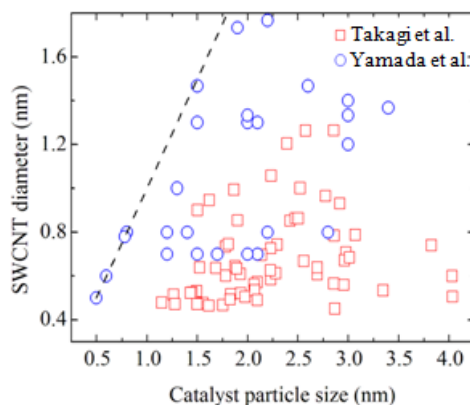
Figure 1. (a) Transmission electron microscopy image of SWCNTs grown using Au nanoparticles. Inset is a scanning electron microscopy image of the sample; (b) Raman spectra (overlain from 20 measurement points) of the sample. The excitation wavelength of the Raman spectra was 785 nm. The peak denoted by * is originated from Si substrate.



Takagi *et al.* first reported SWCNT growth from Au nanoparticles with ethanol as the carbon source [10]. Figure 1 shows electron microscopy images and Raman scattering spectra of G-band and radial breathing modes (RBMs) for the SWCNTs grown using Au nanoparticles. In the transmission electron microscopy image, bundled SWCNTs are seen. In the Raman spectra, G-band near 1600 cm^{-1} is originating from the tangential modes corresponding to vibrations of the carbon-carbon bonds in the plane of the graphene sheet of the SWCNTs. The RBM frequency is inversely proportional to the tube diameter and observable for SWCNTs with a diameter range of 0.4–2 nm [16]. The Au nanoparticles were prepared by vacuum deposition and air-heating of submonolayer Au on silica or aluminum hydroxide substrates. Obtaining Au nanoparticles of 3 nm in diameter or smaller was the key to growing SWCNTs. The Au preparation method did not affect the SWCNT synthesis: they also reported spin-coating of colloidal particles or HAuCl_4 solution [10], and use of Au-filled apo-ferritin (Au-ferritin) [17]. Figure 2 shows the relationship between SWCNT diameter and Au nanoparticle diameter observed on sapphire and quartz substrates using atomic force microscopy (AFM) [10,18]. Those data were obtained from the AFM images of SWCNTs with a catalyst particle at the end. Thus, one by one correspondence was evaluated between diameters of SWCNTs and Au nanoparticles. Although the accuracy of diameter measurement by AFM needs careful examination, the data clearly show a correlation between SWCNT and Au particle diameters. Au particles give the upper bound of SWCNT diameter and most of the SWCNTs are grown from 3 nm or smaller Au nanoparticles.

Bhaviripudi *et al.* also reported SWCNT growth using highly monodisperse Au nanoparticle catalysts prepared by a block copolymer templating technique [12]. The Au-loaded polymer micelle solution was spin-coated onto Si/SiO₂ substrates to form a monolayer of micelles, and the polymeric shell was removed by O₂ plasma treatment. The diameter of the Au nanoparticles was $3.1 \pm 0.4\text{ nm}$. They grew SWCNTs with C₂H₄, CH₄, and H₂ mixture gas at 800 °C.

Figure 2. Size correlation between catalyst nanoparticle and SWCNT. Rectangles and circles represent data in Refs. [10] and [18], respectively.



There are two critical conditions for SWCNT growth using the Au catalyst: the size of the Au particles and pretreatment of them. The particle size for efficient SWCNT growth is smaller than 5 nm, preferably 3 nm or less. Effective pretreatment of Au particles for high SWCNT yields is either air heating or hydrogen heating just before the CVD process [10,19]. The role of pretreatment process might be the removal of hydrocarbon contaminants on the Au particle and exposing the bare Au surface to the carbon source gas. Additionally, heating in air has an effect of preventing agglomeration of the metal particles. This might be due to reduced diffusion of the metal atoms in the oxidation atmosphere. For ion-group catalysts, pretreatment is not critical, probably because hydrocarbon contaminants on the particles can be dissolved into the particles.

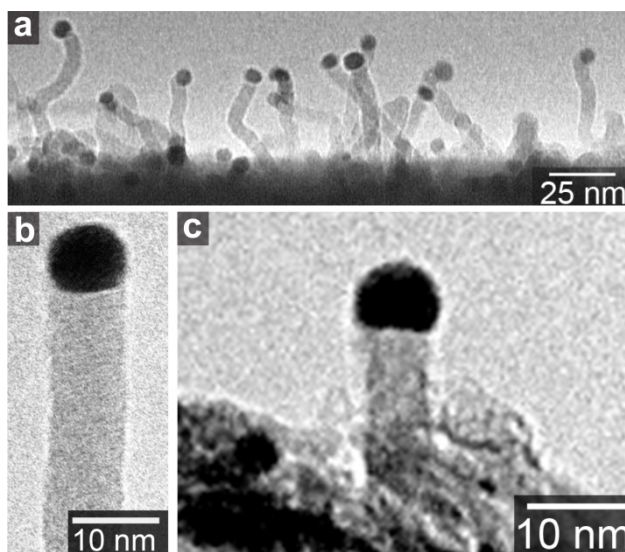
Similar catalytic activity of SWCNT synthesis has been found for Ag and Cu. Takagi *et al.* reported SWCNT growth using Ag and Cu catalysts with the same condition as the Au catalyst: air-heating followed by ethanol CVD at 850 °C [10]. Zhou *et al.*, on the other hand, used CH₄/H₂ mixture gas and grew SWCNTs from Au nanoparticles at 925 °C [11]. Those metals are in the same column in the periodic table and have low solubility of carbon. The growth mechanism of SWCNT should be similar among Au, Ag, and Cu.

Although a wide temperature range (typically, 500–1000 °C) can be employed for growing SWCNTs with iron-group metals, temperatures of 800 °C or higher are used for Au. This is because the absence or moderateness of catalysis for hydrocarbon decomposition. Thus, without an assisting method, such as hot-filament or plasma, a high temperature is necessary to grow SWCNTs. Typical growth temperatures are 850–950 °C for ethanol [10,19,20]. Pyrolysis of ethanol and acetylene takes place in this temperature range. Ghorannevis *et al.* reported use of plasma CVD to enhance SWCNT growth from Au, Pt, and Ag [21]. The carbon source gas was a mixture of methane and hydrogen (H₂) with total pressure of 50 Pa. The growth temperature of SWCNTs was 750 °C, lower than that of thermal CVD. They also reported that the H₂ concentration much affected the yield of SWCNTs from Au, Pt, and Ag, in comparison with the SWCNT growth from the Fe catalyst. They attributed it to the low adsorption efficiency of hydrocarbon species on the Au, Pt, and Ag surfaces: H₂ tends to cause etching of carbon precursors weakly bonded to the catalyst surface.

3. SWCNT Growth Mechanism from Gold Nanoparticles

The basic growth mechanism of SWCNTs from iron-group metals may not far from the VLS picture: carbon bearing molecules in vapor phase are catalytically decomposed on the surface of the catalyst, resulting in the dissolution of carbon atoms into the catalyst particle. Upon supersaturation of carbon concentration in the particle, carbon atoms precipitate from the catalyst, leading to the formation of SWCNTs on the catalyst. However, the catalyst nanoparticles are not necessarily in liquid phase. SWCNT growth from solid catalysts has been confirmed as well as nanowire growth [22,23]. The active forms of Fe catalyst have been reported to be liquid phase, solid Fe metal or Fe carbide depending on the growth temperature and the carbon contamination level [22,24,25]. The Ni catalyst is reported to be in the solid state up to 1200 °C [24]. The point is that carbon uptake into the metal particles and carbon precipitation from the carbon-metal eutectic alloy, *i.e.*, continuous carbon supply from the bulk of the nanoparticle.

Figure 3. (a) Amorphous carbon nanowire grown on SiO₂ substrate in methane ambience at 1100 °C; (b) A magnified image of nanowire in (a); (c) Amorphous carbon nanowire grown on aluminum hydroxide substrate in ethanol ambience at 850 °C [20].



The typical metals of SWCNT growth catalysts, Fe, Co, and Ni, as well as Pd and Pt, have eutectic alloy phase diagrams with carbon. Thus, the VLS-like-mechanism is acceptable for the explanation of SWCNT precipitation from the nanosized metals. On the other hand, Au, Ag, and Cu have low solubility of carbon [26–28]. No chemical reactions or phase transitions of Au particles were observed by *in situ* transmission electron microscopy during MWCNT growth [29]. Nevertheless, these elements also produce SWCNTs. In addition, Au particles around 10 nm produce amorphous carbon wires, as shown in Figure 3 [20]. The carbon nanowires have a gold “cap” on the top of the wire. This shape is similar to a semiconductor nanowire with a gold “cap”, which is believed to be the result of the VLS growth mechanism [14]. Figure 3 suggests that the gold nanoparticles have sizable carbon solubility. Actually, gold has a eutectic alloy phase diagram with carbon, and the carbon solubility in bulk Au at the eutectic point is ~4.7 at.% [26]. Even at such a low content of carbon, the VLS picture could be applied for the C-Au binary system. Furthermore, the carbon solubility becomes higher in

nanoparticles: this is explained by the size effect on the binary alloy phase diagram [7,30]. With decreasing the particle size, melting points of both Au and C decrease [31]. The melting point reduction causes the shift of the phase boundary between liquid (Au + C) and liquid (Au) + solid (C) to higher carbon concentrations [30]. Thus, the carbon solubility in the Au+C droplet, or the carbon concentration at the phase boundary at the CVD temperature, increases with decrease in the Au particle size. Therefore, the VLS mechanism is plausible as the CNT formation mechanism from the Au nanoparticles. On the other hand, for Cu that has a much lower solubility of carbon, the growth mechanism needs further investigation as discussed in section 5.

It should be commented why nanotubes instead of nanowires grow for small nanoparticles. This might be due to the stability of sp^2 carbon networks compared to sp^3 carbon structures such as amorphous carbon or diamond. Okada showed using first-principle total-energy calculations that the outer most shell of a nanowire tends to transform to a sp^2 shell [32,33]. The total energy of a nanowire with 4.3 nm diameter was nearly equal to that of the SWCNT with 1 nm diameter [32]. Structural transformation from nanowire to nanotube, thus, can occur at around 4 nm. This is consistent with the experimental results that SWCNTs were obtained for Au nanoparticles smaller than 5 nm. In addition, the increase of carbon solubility with decreasing Au particle size facilitates the transition from nanowire to nanotube in small Au particles [20]. As the driving force of carbon precipitation from the Au + C droplet is proportional to the concentration difference between the supersaturated carbon in the droplet and equilibrium value at the phase boundary, amorphous carbon wire precipitation is suppressed for smaller Au particles. On the other hand, the increase of the carbon concentration in the particle raises the carbon concentration at the Au particle surface and drives formation of an SWCNT cap on the surface.

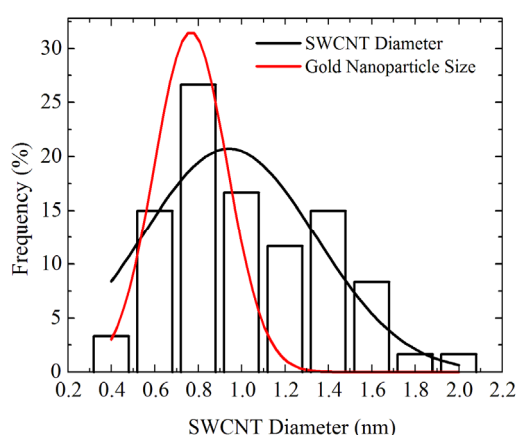
4. Toward the Chirality Control

The properties specific to the Au catalyst compared to iron-group metals are inertness and high vapor pressure in addition to the low carbon solubility. These properties have been utilized for the size and chirality control of grown SWCNTs.

The vapor pressure of bulk Au is approximately 10 times higher than those of iron-group bulk metals [34]. This means that Au particles evaporate much faster than iron-group metal nanoparticles. This feature is useful to reduce the average size only by annealing. Lee and Jeong reported the size change of Au and Fe nanoparticles caused by air heating at 900 °C [35]. The mean diameters of Au nanoparticles decreased from 3.7 ± 0.3 nm to 1.1 ± 0.3 nm during 60 min, annealing at 900 °C, while that of Fe nanoparticles decreased from 2.8 ± 0.8 nm to 2.0 ± 0.4 nm. Obviously, the mean diameter of Au decreased more rapidly than that of the Fe nanoparticles. Yamada *et al.* reported similar results for Au nanoparticles annealed in Ar/H₂ atmosphere. The evolution rate of mean diameter of Au nanoparticles depended on the annealing temperature. Using an appropriate temperature, 850 °C, the mean diameter of ~8 nm decreased to less than 2 nm after 120 min annealing. The evaporation rate of Au nanoparticles was consistent to that of the bulk Au surface of 1.62×10^{-8} g/cm² s at the same temperature [34]. The nanoparticle size thus can be controlled with the temperature comparable to that of CVD. Temperatures as high as 1000 °C are necessary to reduce the size of cobalt nanoparticles [36].

Figure 4 shows diameter distributions of SWCNTs grown using Au nanoparticles obtained by Ar/H₂ annealing at 850 °C [18]. The diameter of the SWCNTs is 0.7–2 nm, which is slightly larger than the diameter distribution of the Au nanoparticles before CVD. The discrepancy of the size distribution between the catalyst particle and SWCNTs can be attributed to the Au particle size change in the CVD ambience. Change in the Au particle size was observed when the ambience was changed from air to Ar/H₂ [18]. Such a size change might be due to the difference of the surface diffusion length depending on the ambience. Therefore, the growth temperature needs to be reduced for keeping the Au nanoparticle size.

Figure 4. Comparison of size distribution between gold nanoparticles annealed for 120 min and SWCNTs [18].



Ghorannevis *et al.* reported narrow chirality distribution of plasma CVD grown SWCNTs [37]. With the assistance of plasma (with methane and H₂ mixture gas), they reduced the growth temperature to 700 °C, at which SWCNT growth from Au nanoparticles did not occur without plasma. In addition, they reported that initial SWCNT growth was attained at 1 min after the sample was exposed to the plasma, whereas 15 min was necessary for the growth of SWCNTs with thermal CVD at the same pressure, 50 Pa. The lower growth temperature and short growth time avoided agglomeration of Au nanoparticles. Furthermore, they found that the H₂ concentration was critical to achieve a narrow chirality distribution of grown SWCNTs. The chirality distribution of grown SWCNTs was evaluated by photoluminescence excitation map [37]. With an optimum H₂ concentration, (6,5) nanotubes became the main chirality obtained. The narrow chirality distribution was also confirmed by absorption spectroscopy and Raman scattering spectroscopy [37]. The (6,5) nanotubes are often obtained from smaller diameter catalyst nanoparticles, implying that the (6,5) nanotube is energetically preferable to other chiralities with similar diameters in the nucleation stage. For the plasma CVD with the Au catalyst, they speculated that since hydrocarbons were weakly bonded with the Au surface, and also H₂ enhanced the etching of carbon precursor on the catalyst surface, the growth of larger diameter SWCNTs are strongly suppressed [21,37].

5. Comparison with Graphene Synthesis

Graphene is known to segregate on the surface of transition metals such as Ni, Co, Pd, and Pt, as a result of carbon precipitation from the bulk [3]. Those metals are also used as the substrate of graphene CVD. On the other hand, Cu has very low carbon solubility, yet graphene is synthesized on the Cu surface by CVD [13]. The graphene growth is mediated by surface diffusion of carbon atoms on the Cu surface, and lack of carbon precipitation from the bulk facilitates the monolayer graphene growth. Li *et al.* clearly showed that graphene growth on Cu was dominated by surface adsorption of CH₄ by using carbon isotope labeling and Raman imaging, whereas that on Ni was promoted by dissolution and segregation of carbon from the bulk [38]. This is interesting when we compare it with SWCNT growth. For the case of Au, as shown in the previous section, SWCNT growth from Au nanoparticles is thought to be mediated by the VLS-like mechanism. However, if the effect of carbon precipitation from the Cu nanoparticle is negligible, SWCNT growth should be promoted only by the carbon atoms on the Cu nanoparticle surface. This is a surface growth model, which also explains SWCNT growth from nonmetal particles, such as alumina and nanodiamond [39,40]. The differences between the graphene growth and SWCNT growth are the curvature of the catalyst surface and the volume of the metal. The underlying mechanism should be the same. Thus, the understanding of graphene growth on the flat metal surfaces will contribute to elucidation of the SWCNT formation mechanism on the nanoparticle surface. Thus far, graphene growth on the pure Au surface has not been reported, but it should be possible. Weatherup *et al.* reported use of a Au-Ni alloy as the substrate of graphene CVD [41]. On the Au-Ni alloy catalyst surface, a uniform graphene film with fewer layers and larger domain sizes was obtained by exposing to C₂H₂ at 450 °C in contrast to inhomogeneous multilayered graphene domains on the Ni surface.

6. Summary

Gold nanoparticles smaller than 5 nm catalyze the synthesis of SWCNTs in chemical vapor deposition. Gold is an inert metal but its eutectic alloy with silicon or germanium has been known to produce whiskers or nanowires, which is understood as the vapor-liquid-solid mechanism. A similar mechanism seems to contribute to the growth of SWCNTs from gold nanoparticles in spite of the low solubility of carbon in gold. Different from semiconductor nanowires, carbon atoms form tubular structure for gold nanoparticles smaller than 5 nm. This can be attributed to the stability of sp² carbon networks compared to sp³ carbon structures. The inertness and high vapor pressure of gold is utilized for the diameter and chirality control of SWCNTs. Cu and Ag also catalyze the synthesis of SWCNTs, but details of the growth mechanism with these metals need to subject further investigations.

Conflicts of Interest

The author declares no conflict of interest.

References

1. Geim, A.K.; Novoselov, K.S. The rise of graphene. *Nat. Mater.* **2007**, *6*, 183–191.

2. Iijima, S.; Ichihashi, T. Single-shell carbon nanotubes of 1-nm diameter. *Nature* **1993**, *363*, 603–605.
3. Wintterlin, J.; Bocquet, M.-L. Graphene on metal surfaces. *Surf. Sci.* **2009**, *603*, 1841–1852.
4. Kong, J.; Cassell, A.M.; Dai, H. Chemical vapor deposition of methane for single-walled carbon nanotubes. *Chem. Phys. Lett.* **1998**, *292*, 567–574.
5. Hamilton, J.C.; Blakely, J.M. Carbon segregation to single crystal surfaces of Pt, Pd and Co. *Surf. Sci.* **1980**, *91*, 199–217.
6. Gavillet, J.; Loiseau, A.; Journet, C.; Willaime, F.; Ducastelle, F.; Charlier, J.C. Root-growth mechanism for single-wall carbon nanotubes. *Phys. Rev. Lett.* **2001**, *87*, 275504.
7. Harutyunyan, A.R.; Mora, E.; Tokune, T.; Bolton, K.; Rosén, A.; Jiang, A.; Awasthi, N.; Curtarolo, S. Hidden features of the catalyst nanoparticles favorable for single-walled carbon nanotube growth. *Appl. Phys. Lett.* **2007**, *90*, 163120.
8. Saito, Y.; Nishikubo, K.; Kawabata, K.; Matsumoto, T. Carbon nanocapsules and single layered nanotubes produced with platinum group metals (Ru, Rh, Pd, Os, Ir, Pt) by arc discharge. *J. Appl. Phys.* **1996**, *80*, 3062–3067.
9. Raty, J.Y.; Gygi, F.; Galli, G. Growth of carbon nanotubes on metal nanoparticles: a microscopic mechanism from ab initio molecular dynamics simulations. *Phys. Rev. Lett.* **2005**, *95*, 096103.
10. Takagi, D.; Homma, Y.; Hibino, H.; Suzuki, S.; Kobayashi, Y. Single-walled carbon nanotube growth from highly activated metal nanoparticles. *Nano Lett.* **2006**, *6*, 2642–2645.
11. Zhou, W.; Han, Z.; Wang, J.; Zhang, Y.; Jin, Z.; Sun, X.; Zhang, Y.; Yan, C.; Li, Y. Copper catalyzing growth of single-walled carbon nanotubes on substrates. *Nano Lett.* **2006**, *6*, 2987–2990.
12. Bhaviripudi, S.; Mile, E.; Steiner, S.A.; Zare, A.T.; Dresselhaus, M.S.; Belcher, A.M.; Kong, J. CVD synthesis of single-walled carbon nanotubes from gold nanoparticle catalysts. *J. Am. Chem. Soc.* **2007**, *129*, 1516–1517.
13. Li, X.; Cai, W.; An, J.; Kim, S.; Nah, J.; Yang, D.; Piner, R.; Velamakanni, A.; Jung, I.; Tutuc, E.; *et al.* Large-area synthesis of high-quality and uniform graphene films on copper foils. *Science* **2009**, *324*, 1312–1314.
14. Wagner, R.S.; Ellis, W.C. Vapor-liquid-solid mechanism of single crystal growth. *Appl. Phys. Lett.* **1964**, *4*, 89–90.
15. Lee, S.-Y.; Yamada, M.; Miyake, M. Synthesis of carbon nanotubes over gold nanoparticle supported catalysts. *Carbon* **2005**, *43*, 2654–2663.
16. Jorio, A.; Dresselhaus, M.; Saito, S.; Dresselhaus, G.F. *Raman Spectroscopy in Graphene Related Systems*; Willy-VCH: Weinheim, Germany, 2011; pp. 199–220.
17. Takagi, D.; Yamazaki, A.; Otsuka, Y.; Yoshimura, H.; Kobayashi, Y.; Homma, Y. Gold-filled apo-ferritin for investigation of single-walled carbon nanotube growth on substrate. *Chem. Phys. Lett.* **2007**, *445*, 213–216.
18. Yamada, K.; Kato, H.; Homma, Y. Narrow diameter distribution of horizontally aligned single-walled carbon nanotubes grown using size-controlled gold nanoparticles. *Jpn. J. Appl. Phys.* **2013**, *52*, 035105.

19. Liu, H.; Chokan, T.; Takagi, D.; Ohno, H.; Chiashi, S.; Homma, Y. Effect of ambient gas on the catalytic properties of Au in single-walled carbon nanotube growth. *Jpn. J. Appl. Phys.* **2008**, *47*, 1966–1970.
20. Takagi, D.; Kobayashi, Y.; Hibino, H.; Suzuki, S.; Homma, Y. Mechanism of gold-catalyzed carbon material growth. *Nano Lett.* **2008**, *8*, 832–835.
21. Ghorannevis, Z.; Kato, T.; Kaneko, T.; Hatakeyama, R. Growth of single-walled carbon nanotubes from nonmagnetic catalysts by plasma chemical vapor deposition. *Jpn. J. Appl. Phys.* **2010**, *49*, 02BA01.
22. Yoshida, H.; Takeda, S.; Uchiyama, T.; Kohno, H.; Homma, Y. Atomic-scale *in-situ* observation of carbon nanotube growth from solid state iron carbide nanoparticles. *Nano Lett.* **2008**, *8*, 2082–2086.
23. Kodambaka, S.; Tersoff, J.; Reuter, M.C.; Ross, F.M. Germanium nanowire growth below the eutectic temperature. *Science* **2007**, *316*, 729–732.
24. Rao, R.; Pierce, N.; Liptak, D.; Hooper, D.; Sargent, G.; Semiatin, S.L.; Curtarolo, S.; Harutyunyan, A.R.; Maruyama, B. Revealing the impact of catalyst phase transition on carbon nanotube growth by *in situ* raman spectroscopy. *ACS Nano* **2013**, *7*, 1100–1107.
25. Wirth, C.T.; Bayer, B.C.; Gamalski, A.D.; Esconjauregui, S.; Weatherup, R.S.; Ducati, C.; Baetz, C.; Robertson, J.; Hofmann, S. The phase of iron catalyst nanoparticles during carbon nanotube growth. *Chem. Mater.* **2012**, *24*, 4633–4640.
26. Okamoto, H.; Massalski, T.B. The Au-C (gold-carbon) system. *Bull. Alloy Phase Diagrams* **1984**, *5*, 378–379.
27. Hansen, M.; Anderko, K. *Constitution of Binary Alloys*; McGraw-Hill: New York, NY, USA, 1958.
28. Oden, L.L.; Gokcen, N.A. Cu-C and Al-Cu-C phase diagrams and thermodynamic properties of C in the alloys from 1550 °C to 2300 °C. *Metall. Mat. Trans. B* **1992**, *23*, 453–458.
29. Tang, D.-M.; Liu, C.; Yu, W.-J.; Zhang, L.-L.; Hou, P.-X.; Li, J.-C.; Li, F.; Bando, Y.; Golberg, D.; Cheng, H.-M. Structural changes in iron oxide and gold catalysts during nucleation of carbon nanotubes studied by *in situ* transmission electron microscopy. *ACS Nano* **2014**, *8*, 292–301.
30. Tanaka, T.; Hara, S. Thermodynamic evaluation of nano-particle binary alloy phase diagrams. *Z. Metallkd.* **2001**, *92*, 1236–1241.
31. Wautelet, M. Estimation of the variation of the melting temperature with the size of small particles on the basis of a surface-phonon instability model. *J. Phys. D* **1991**, *24*, 343–346.
32. Okada, S. Formation of graphene nanostructures on diamond nanowire surfaces. *Chem. Phys. Lett.* **2009**, *483*, 128–132.
33. Okada, S.; Takagi, Y.; Kawai, T. Formation of multi-walled nanotubes from diamond nanowires. *Jpn. J. Appl. Phys.* **2010**, *49*, 02BB02.
34. Lide, D.R. *CRC Handbook of Chemistry and Physics*, 75th ed.; CRC Press: Boca Raton, FL, USA, 1994; pp. 4-124–4-125.
35. Lee, S.-H.; Jeong, G.-H. Effect of catalytic metals on diameter-controlled growth of single-walled carbon nanotubes: Comparison between Fe and Au. *Electron. Mater. Lett.* **2012**, *1*, 5–9.
36. Jeong, G.H.; Suzuki, S.; Kobayashi, Y.; Yamazaki, A.; Yoshimura, H.; Homma, Y. Size control of catalytic nanoparticles by thermal treatment and its application to diameter control of single-walled carbon nanotubes. *Appl. Phys. Lett.* **2007**, *90*, 043108.

37. Ghorannevis, Z.; Kato, T.; Kaneko, T.; Hatakeyama, R. Narrow-chirality distributed single-walled carbon nanotube growth from nonmagnetic catalyst. *J. Am. Chem. Soc.* **2010**, *132*, 9570–9572.
38. Li, X.; Cai, W.; Colombo, L.; Ruoff, R.S. Evolution of graphene growth on Ni and Cu by carbon isotope labeling. *Nano Lett.* **2009**, *9*, 4268–4272.
39. Takagi, D.; Kobayashi, Y.; Homma, Y. Carbon nanotube growth from diamond. *J. Am. Chem. Soc.* **2009**, *131*, 6922–6923.
40. Liu, H.; Takagi, D.; Ohno, H.; Chiashi, S.; Chokan, T.; Homma, Y. Growth of single-walled carbon nanotubes from ceramic particles by alcohol chemical vapor deposition. *Appl. Phys. Express* **2008**, *1*, 014001.
41. Weatherup, R.S.; Bayer, B.C.; Blume, R.; Ducati, C.; Baetz, C.; Schlögl, R.; Hofmann, S. *In situ* characterization of alloy catalysts for low-temperature graphene growth. *Nano Lett.* **2011**, *11*, 4154–4160.

© 2014 by the authors; licensee MDPI, Basel, Switzerland. This article is an open access article distributed under the terms and conditions of the Creative Commons Attribution license (<http://creativecommons.org/licenses/by/3.0/>).